Dealing with uncertainty in the probability of overtopping of a flood mitigation dam

Eleni Maria Michailidi and Baldassare Bacchi
DICATAM, Università degli studi di Brescia, Via Branze 42, 25123 Brescia, Italy
Correspondence to: E. M. Michailidi (e.michailidi@unibs.it)

Abstract. In recent years, copula multivariate functions were used to model, probabilistically, the most important variables of flood events: discharge peak, flood volume and duration. However, in most of the cases the sampling uncertainty, from which small-sized samples suffer, is neglected. In this paper, considering as a case study a real reservoir controlled by a dam, we apply a structure-based approach to estimate the probability of reaching specific reservoir levels, taking into account the key components of an event (flood peak, volume, hydrograph shape) and of the reservoir (rating curve, volume-water depth relation). Additionally, we improve information about the peaks from historical data and reports through a Bayesian framework, allowing the incorporation of supplementary knowledge from different sources and its associated error. As it is seen here, the extra information can result in a very different inferred parameter set and consequently this is reflected as a strong variability of the reservoir level, associated with a given return period. Most importantly, the sampling uncertainty is accounted for in both cases (single site and multi-site with historical information) and Monte Carlo confidence intervals for the maximum water level are calculated. It is shown that water levels of specific return periods in a lot of cases overlap, thus making risk assessment without providing confidence intervals deceiving.

1 Introduction

In the relatively recent literature there is a wide application of the copula functions to model the natural variability of hydrometeorological variables, ranging from rainfall (De Michele and Salvadori, 2003; Zhang and Singh, 2007; Balistrocchi and Bacchi, 2011; Singh and Zhang, 2007; Ariff et al., 2012) to floods (Aronica et al., 2012; Balistrocchi et al., 2014; Candela et al., 2014; Domeneghetti et al., 2013; Gräler et al., 2013; Ganguli and Reddy, 2013).

An important application of this multivariate analysis is the determination of the risk of failure of a hydraulic structure. De Michele et al. (2005) were the first to check the adequacy of a dam's spillway under a bivariate hydrological load, followed by Requena et al. (2013), while Volpi and Fiori (2014) formalised the idea that the return period of a failure of a structure depends on the structure of interest and therefore the interaction between the hydrological loads and the structure should be taken into consideration by fixing a "structure-based" return period.

In the same conceptual framework, Serinaldi (2016) suggested that the choice between a univariate and multivariate risk assessment should not be based on whether one or the other over/under estimate the risk but rather on the operational criteria of the problem, or simpler on what is the mechanism of failure.

Copulas are functions that combine marginal distributions to the joint cumulative distribution, therefore the latter is only indirectly affected by the choice of the marginals. So, the practical problem of identification and estimation of the joint distribution is handled from two non-interwinding aspects; the dependence structure of the set of variables and the marginal distributions.

In the majority of the studies, the communication of the sampling uncertainty- an integral component in a univariate framework- is overlooked in a multivariate case. Serinaldi (2013) studied the effect of sample size on the confidence bands of the probability of exceedance curves of a joint peak-volume event and showed that in small and medium sample sizes these curves largely overlap. Similarly, Zhang et al. (2015) implemented a Bayesian inference approach to account for the uncertainty of parameter estimation and for the occurrence of a drought, coming to the conclusion that the 95 % confidence interval of a 20-year event can include the expected values of 10 up to 50-year events.

In order to account for the sampling uncertainty of multivariate cases, where a variable of interest can be expressed as a function of one or more variables, Serinaldi (2016) proposed a Monte Carlo procedure. He also underlined the importance of including confidence intervals when providing point estimates of the variable of interest, which is even more necessary in the multivariate frequency analysis, where the unknown dependence structure contributes to the uncertainty.

The sampling uncertainty in a joint peak-volume event was quantified by Dung et al. (2015) who used two bootstrapping methods- one developed by the authors and the second by Serinaldi (2013)- and concluded, as the previous, that the model selection and parameter estimation methods is of minor significance in uncertainty estimation in respect with sampling uncertainty, even in relatively large sample sizes. They suggested that efforts should be focused on the expansion of the data set in order to achieve a reduction of uncertainty.

The data expansion can be temporal, spatial and causal (Merz and Blöschl, 2008), thus enriching the available evidence with information from neighbouring basins, previous periods and by comprehension of the flood-generating mechanisms. In the past, many researchers (Parent and Bernier, 2003; Reis Jr and Stedinger, 2005; Gaume et al., 2010; Halbert et al., 2016; Parkes and Demeritt, 2016; Viglione et al., 2013) have dealt with the extension of the available data using information on paleo-floods, historical flood reports, marks of the river stage during important flood events, expert judgement etc. with the aim of reducing the range of uncertainty bands or simply to reach a more realistic design value. Bayesian inference allows the integration of information from different sources and their associated uncertainty and errors and provides a mean of conveying hydrological reasoning in a mathematical context.

In this research we validate a methodology of flood risk assessment in a real case-study, where risk is expressed in terms of probability of exceeding a given reservoir level in an on-line flood mitigation dam. We consider this level as a function of flood peak, volume and hydrograph shape and, consequently, multivariate modelling is implemented with the use of copulas. The characteristics of the reservoir- also a function of the level- are synthesised in the rating curve and the volume-level curve. The main scope is to integrate the associated sampling uncertainty and to build confidence intervals for each water level through Monte Carlo simulations. Furthermore, we incorporate additional information on the peaks in a Bayesian framework and we examine its effect on the distributions, their confidence intervals, as well as the ones of the reservoir level frequency curve.

2 Case study and data

We have focused our interest on the Panaro catchment- an important influent of Po river in Northern Italy. In particular, the watershed under investigation is composed by the Panaro river itself, the Scoltenna and the Leo tributaries with an outlet upstream of the Panaro dam (Fig. 1) and occupies an area of 876 km^2. Panaro has its source at Monte Cimone (2.165 m a.s.l.) and flows into Po, at Bondeno; It takes its name at the valley of Montespecchio after converging with the Leo and Scoltenna streams, that constitute the upper part of the river network. The hydrographic network of the watershed shows a low degree of hierarchy, indicating an evolving state which is also evident by the existence of torrential dynamic phenomena (Autorità di bacino del fiume Po, 2006).

The influence of snowfall is negligible due to the modest land elevation and the majority of rainfall events occur seasonally (September-April). The average precipitation height ranges between 700 and 2000 mm/year (Autorità di bacino del fiume Po, 2006).

The basin's permeability is low and therefore the runoff is influenced little by water infiltration. In fact, the study basin consists mostly of sandstones and silicatic alternating sequences (44 % of total area) and marls and clay (34 %).

The Panaro dam is a concrete gravity dam (150 m in length), located near the city of Modena and constructed for flood mitigation purposes. The hydraulic system consists of two reservoirs, a principal on the river course and a secondary at the right river bank, and a series of levees that enclose them. The crest of the principal levees are at 44.85 m a.s.l.. The reservoirs can hold in total 23.66 hm^3 up to the spillway's crest at 41.1 m a.s.l.. There are also nine discharge outlets at the bottom of the dam that ensure constant flow to the downstream valley.

The available flood data included a 52-year discharge series (1936-1943,1945 and 1946 were missing) with an hourly time interval from the Bomporto station located downstream, near the current location of the dam. The hydrological characteristics of the study basin are briefly presented in Table 1.

Additional data included the annual peaks of the missing years from the same station (Servizio Idrografico Italiano, 1939,1953) and recent annual peaks from upstream stations, after consulting the annual hydrological reports of ARPA- Emilia Romagna published in its website (www.arpae.it); in specific for 2003 from Pievepelago, for 2004, 2005 and 2015 from Ponte Samone, and for 2006 to 2014 from Spilamberto.

In a report about natural disaster risks in the city of Modena (Nora and Ghinoi, 2009) it is also stated that the most disastrous flood events of the 20th century happened during the last 40 years (1966, 1969, 1972 and 1973). In November 1966 the flooded area from the Panaro covered $9400\ \mathrm{ha}$, in September 1972 $2540\ \mathrm{ha}$ and in September 1973 $6000\ \mathrm{ha}$ (Nora and Ghinoi, 2009).

3 Methodology

3.1 Data regionalisation

In order to rescale the flood information from subcatchments and from the downstream station, depending on the area, the following scale function was used:

$$Q(A_1) = Q(A_2)(A_1/A_2)^m \tag{1}$$

where $Q(A_1)$ is the rescaled discharge, $Q(A_2)$ a known discharge and m a regional scale exponent.

De Michele and Rosso (2002) clustered basins with similar flood generation mechanism and checked the homogeneity of the grouped regions. The study area was located in North-western Italy and included the Panaro watershed. The proposed scale exponent m for this region is 0.772 with a standard deviation of 0.072. In our case the rescaling regarded different locations of the same basin, although in theory neighbouring basins could have been used (e.g Secchia), but they did not add additional information here.

3.2 Incorporating additional data

Thomas Bayes' theorem expresses how an individual's degree of belief can change after the presence of new evidence. Bayes' theorem can be formulated as:

$$p(\theta \mid D) = \frac{l(D \mid \theta)\,\pi(\theta)}{\int l(D \mid \theta)\pi(\theta)d\theta} \propto l(D \mid \theta)\,\pi(\theta) \tag{2}$$

where $\pi(\theta)$ is the prior density distribution of the parameters θ, $p(\theta \mid D)$ is the posterior distribution after the introduction of the observed information D and $l(D \mid \theta)$ is the likelihood of the data. The denominator serves only as a normalisation constant to ensure unity of the area under $p(\theta \mid D)$, so the equality sign can be substituted with the proportionality sign. This integral cannot be solved analytically, so for its computation Monte Carlo Markov Chain algorithms are employed. In each Markov chain the aim is the maximisation of the logarithm of the unnormalised joint posterior distribution starting from an initial value and proceeding iteratively in order to arrive at each target distribution (Statisticat, LLC, 2016).

In a Bayesian framework the model's parameters are handled as stochastic variables in order to incorporate the uncertainty of their values (Ouarda and El-Adlouni, 2011). In the present case the model's parameters were the parameter of the peak marginal distribution and the scale exponent. We used non-informative prior distribution for the marginal and a normal distribution prior for the exponent $m \backsim N(0.772, 0.072)$. We integrated a perception threshold X_P- a value which only in k number of years in a historic period of h years was exceeded; here it is set as at about $1000\ \mathrm{m}^3/\mathrm{s}$, a value thought to be exceeded only once in a historic period of 117 years since flood reports indicate that during the early years of 1900s, when systematic records were non-existent, the flood events were of less significance in comparison with the events occurring at the $70s$. Additionally we have introduced the uncertainty of the scale exponent m. Therefore, the likelihood function of the data is set as:

$$l(D \mid \theta) = \begin{bmatrix} h \\ k \end{bmatrix} F_X(X_P)^{(h-k)} \prod_{i=1}^{s} [\prod_{j=1}^{n_i} f_x(y_{ij}(A/A_i)^m)] \tag{3}$$

where $\begin{bmatrix} h \\ k \end{bmatrix} = \frac{h!}{k!(h-k)!}$ is the binomial coefficient, s is the number of different sites of the recorded flood peaks, n_i is the number of recorded peaks for each site, y_{ij} are the annual peaks from the different sites.

The Bayesian inference was conducted in R with the package LaplacesDemon (Statisticat, LLC, 2016) and the MCMC algorithm utilised was the Componentwise Hit-And-Run Metropolis. The logarithm of the posterior distribution to be maximised is the sum of the logarithm of the likelihood and the logarithm of the priors:

$$log(p(\mu,\sigma,m \mid D) = log(l(D \mid \mu,\sigma,m) + log(\pi(m)) \tag{4}$$

where μ and σ are the mean and shape parameters of the peak distribution.

3.3 Copula and marginal inference

Copulas are functions that describe the dependence structure between variables independently of the choice of marginal distributions. The joint distribution functions and the marginals are linked by Sklar's theorem (Sklar, 1959):

$$F(x_1,...,x_d) = C(F_1(x_1),...,F_d(x_d)) \tag{5}$$

for all $\mathbf{x} \in R^d$, where the F_i, $i = 1,...,d$ are the marginals of F and C is the copula function.

Copulas provide a powerful tool for the statistical modelling of multivariate data: for a theoretical introduction see Nelsen (2006); Joe (2014); Durante and Sempi (2015), for a practical engineering approach see Genest and Favre (2007); Salvadori et al. (2007); Salvadori and De Michele (2007).

The application of copula functions has facilitated overcoming some inadequacies of traditional multivariate distributions such as that the marginals must derive from the same distribution family and their parameters may define the dependence structure between the variables (Salvadori et al., 2007).

The degree of relation between pairs of variables was examined by measures of association. These include Kendall's τ, Spearman's ρ_S which express the existence or absence of concordance and Pearson's ρ_P which expresses linear dependence. For the observed discharge/volume pairs these were equal to 0.58, 0.77 and 0.81, accordingly and indicate strong dependence.

In the absence of a long sample, the copulas that fit the data can be numerous and goodness-of-fit tests cannot distinguish between them (Serinaldi, 2013). Since inferring the "correct" copula model is not the aim of this research and since this endeavour at this point can be futile, given the available data set, the final choice was based partly on the preference of previous published research towards the Gumbel, including conference proceedings by Balistrocchi et al. (2014) who fitted the Gumbel on peaks obtained from a Peak-Over-Threshold method on the same discharge time series. In the present case both the Gaussian and the Gumbel-Hougaard one-parameter copula passed the goodness-of-fit tests (Cramer-von Mises and Kolmogorov-Smirnov) and demonstrated the smallest Akaike weights- or else the probability that the chosen model is the most apt among the tested ones (Burnham and Anderson, 2004). However, we thought that if tail-dependence exists, Gumbel would be more appropriate (belonging to the extreme value copula family), as the Gaussian has no tail dependence. We recall the

Gumbel-Hougaard copula as:

$$C(u,v) = \exp[-((-\log(u))^{\theta} + (-\log(v))^{\theta})^{1/\theta} \quad (6)$$

where u, v are the pseudo-observations and θ the copula parameter.

The existence of tail dependence between peak and volume was also implied by some historical evidence. Many significant events in Italy occur when a frontal perturbation, generated by the cold high masses coming from the North Atlantic Ocean or the Arctic Ocean, meets Mediterranean southward warm fronts. Depending on the persistence of the south and north current, the generated front begins to develop covering a large area (e.g. 10^4 km^2). Inside this warm front, the energy content is very high. This causes local convective phenomena enhanced by orographic effects. So, thunderstorms can appear locally producing rainfall whose values can surpass one third of the mean annual in 24-30 hours. In the vicinity of the local thunderstorms the rainfall is moderately high producing large soil saturation and increasing, significantly, the contribution to the groundwater. This kind of rainfall events produces not only maximum observed peaks of flood in many rivers of small (<100 km^2) and medium size (<2000 km^2) but also the largest observed volumes associated with the persistence of the global event. This is the case, for example, for the flood in Florence and Triveneto on 4th November 1966, in Valtellina on 18-25th July 1987, along Tanaro on 5-6th November 1994, along Po in Piedmont on 17-21st October 2000, etc.

Unfortunately, tail dependence estimators such as the ones of Frahm et al. (2005) and Schmidt and Stadtmüller (2006) can be biased and susceptible to high uncertainty even in large sample sizes (Serinaldi et al., 2015), thus their use in this case is discouraged.

Regarding the choice of the marginal distributions, we preferred distributions that were more parsimonious, thus reducing the additional statistical uncertainty introduced by an extra parameter, following the logic of Occam's razor, and that provided a nice visual fit. The differences between the corrected AIC, BIC and Akaike weighted values were not sufficient to make a safe distinction between the models. The peaks were modelled with the Inverse Gaussian distribution (two parameters instead of three of the GEV) and their corresponding volumes with the one-parameter Rayleigh. It is, however, imperative to note that there was no clear indication of overall performance superiority of the chosen distributions.

The parameters of the inferred distributions (copula and marginals) are presented in Table 2.

3.4 Hydrograph selection

The shape of the "design hydrograph" is often considered an important factor in the design procedure and is related to the spatial and temporal rain distribution as well as the basin's shape and behaviour (Singh, 1997). Therefore typical hydrographs were determined from the annual maxima flood events extracted from the available time series. In particular, the events' hydrographs were clustered according to their characteristics and utilizing the methodology proposed by Dyck and Peschke (1995) which suggests the normalisation of the hydrograph (after the removal of the baseflow) by

$$Q_{norm} = (Q - q_{base})/(Q_{max} - q_{base}) \quad (7)$$

$$t_{norm} = t/t_{Qmax} \tag{8}$$

where Q_{max} the hydrograph's peak, q_{base} the base flow and t_{max} the time to peak, starting from the rising limb of the flood event.

Consequently, the normalised peak equals to one at time 1. All normalised hydrographs were extended to a common duration (for comparison purposes) and cluster analysis with the Ward method and Euclidean distances was implemented (Aronica et al., 2012).

3.5 Structure-based risk analysis

Volpi and Fiori (2014) associated the return period with the structure of interest by relating the structure design parameter to the hydrological load through the function $Z = g(\mathbf{X})$. Consequently the structure-oriented return period of a value z takes the form:

$$T_{STR} = \frac{\mu_T}{1 - F_Z(z)} \tag{9}$$

where μ_T is the mean interarrival time between two consecutive occurrences of z (in our case $\mu_T = 1$ year), F_Z is the probability distribution function of the derived variable Z, which in this case is the reservoir level and $\mathbf{X} \equiv (Q, V, shape, ...)$. Here, the structure function is very complex, since the reservoir level is a function of the spillway's rating curve and the flood's natural variables, and therefore the whole analysis must be based on Monte Carlo simulations. This adds to the computational burden, specifically when dealing with the quantification of the uncertainty.

3.6 Uncertainty estimation

In order to account for sampling uncertainty and to estimate the confidence intervals the following Monte Carlo procedure was implemented, originally proposed by Serinaldi (2016).

1. Estimate the parameter $\hat{\theta}$ of the copula for the observed sample as well as the parameter of the flood volume distribution.
2. Simulate B bivariate samples of size n (equal to the number of years of the observed sample) using the estimated copula parameter and then transform into volume using the estimated parameter of the marginal.
3. Calculate the copula parameter $\hat{\theta}$ and the volume marginal parameter for each sample with the same estimation method used for the observed sample.
4. Simulate B bivariate samples of size M with the copula parameter $\hat{\theta}$ estimated in the previous step.
5. Transform the samples from the unit interval to discharge and volume using the estimated marginal parameters. Generate $B \times M$ hydrographs with an assigned peak, volume and shape and route them to calculate the reservoir level and the frequency curves of all B samples.

6. Build the confidence intervals of the reservoir level frequency curves.

In the present research B was set equal to 10000 and M equal to 1000.

The confidence intervals of the peaks marginal distribution parameters have been estimated in a Bayesian framework, as stated previously, in order to incorporate the additional knowledge and to account for the scaling uncertainty.

The parameter uncertainty of additional distributions that fit the data could be introduced in the procedure, leading in larger confidence intervals. However, in this case, only the parameter uncertainty of the inferred models was of interest.

4 Results and discussion

Initially we have clustered the hydrograph shapes into four characteristic groups. After simulating 10000 peak-volume pairs from the inferred distributions, we assigned to each one a specific hydrograph shape (respecting their frequency of occurrence). Then, we denormalised and routed the hydrographs; we repeated the same procedure but after clustering into only one group, thus considering a global "mean" hydrograph. The characteristic shapes are depicted in Fig. 2a, along with the "mean" shape (Fig. 2b). The level frequency curve showed small differences between the two cases (Fig. 3) and as we shall see later this difference is negligible in comparison with the estimated uncertainty. So, we have proceeded with the uncertainty assessment considering one "mean" hydrograph.

We have implemented the Bayesian framework on the peaks extracted from the systematic discharge series recorded at Bomporto station, adding also the uncertainty of the scaling exponent of the regionalisation relation. In the second scenario, we also included recently recorded annual peaks from other hydrometric stations of the same basin, mentioned previously, as well as information from flood reports, while integrating the uncertainty of the scaling exponent. As it can be seen in Fig. 4, when ignoring the additional information, the estimate of discharge peak is lower for a given return period. We focus our attention on relatively small return periods since any extrapolation beyond the available time period is subject to great uncertainty. Indicatively, a peak with a univariate return period of 50 years can increase by 18%, exceeding the confidence intervals of the fitted distribution. This occurs because during the last 10 years crucial flood events appeared in the area. In Table 2 we note that in the second case the distribution's mean is bigger and the shape parameter is smaller with a significantly lower standard deviation.

The 95 % confidence interval of both of the peak distributions can be wide (Fig. 4), e.g. for a univariate return period of 50 years it can span from 665 to 941 m^3/s (29 % difference) and from 837 to 1092 m^3/s (23 % difference) for the first and second case.

Similarly, in the case of the flood volume the 95 % confidence interval for a univariate return period of 50 years can span from 95.5 to 120 hm^3 (20 % difference) (Fig. 5).

The confidence intervals of the parameters of the inferred distributions are presented in Table 2.

The results of the increased peaks are reflected also on the frequency curve of the maximum water level (MWL). The return period here corresponds to a water level, so it is considered structure-based, since the level is a function of the structural and operational characteristics of the dam, among others. As it can be seen (Fig. 6), the MWL is significantly lower in the case of

no extra information, especially for greater return periods. For a return period of 50 years the average MWL can differ 1.2 m- a considerable magnitude in terms of volume and when considering that the safety margin above the spillway's crest is in some cases 1 m.

In Fig. 7 highest density regions depict a sort of confidence intervals of the MWL for specific return periods for each case (single site information & multi-site with historical information). These regions can be defined as the smallest areas in the sample space with a certain probability coverage and they have the advantage of displaying multimodal distributions, thus they may consist of disjoint subsets (Hyndman, 1996). They are particularly suitable in multivariate cases or for asymmetrical distributions. In the HDR boxplots the mode (horizontal line) substitutes the median and the darker region corresponds to a probability coverage of 50 %, the lighter to a coverage of 95 % and the points outside to the data beyond the 95 % probability.

The span of the highest density regions slightly decreases as more information is introduced. However, this decrease in uncertainty seems small and we cannot conclude whereas the extra information has contributed to a systematic uncertainty reduction. An increase in the simulation size could lead to a slightly different picture, however the added computational burden is prohibitive and anyhow, as Salvadori et al. (2015) stated, a clear rule-of-thumb regarding the simulation size does not exist. In any case the size is considered large enough for some safe conclusions, especially for the smaller return periods.

Within a certain return period the parameter uncertainty can lead to substantial MWL variations, e.g. for 20 years (in the case of extra information), the span of the MWL with a density of 50 % and 95 % is of 0.8 and 2.3 m, accordingly, which correspond to huge volume differences. These can have devastating effects not only in the case of overtopping but also because the remaining water can cause bank failure due to piping. These spans could increase for larger return periods, where the uncertainty is bound to get vaster.

As the results of previous studies suggested (Serinaldi, 2013; Dung et al., 2015; Zhang et al., 2015; Serinaldi, 2016), the regions of the return periods can overlap; in this case the 95 % confidence interval of an event of 20 years can include, marginally, the expected values of events of 10 up to 50 years (e.g. single-site scenario). For the multi-site with extra information scenario the overlapping region is smaller.

In Fig. 8 the highest density regions (50, 75 & 95 %) are depicted in a two-dimensional plane (discharge-volume) that correspond to a return period of 50 years. For events that result in a MWL with a specific return period, the variation of discharge and volume can be huge even when looking in the smaller density regions (e.g. 50 %). For example, in the 95% region the discharge can assume values with a univariate return period from 1 to 50 years (for the multi-site scenario), which is a strong indicator of the non-linearity of the problem. The same applies for the flood volume.

5 Conclusions

This analysis focuses on the uncertainty introduced when calculating the probability of exceeding specific water levels in a flood control reservoir, which is a result of the parameter uncertainty of the marginals of the hydrological variables, as well as the copula multivariate function, due to the small size that characterises in most cases a hydrological sample. Therefore, we attempted to quantify this uncertainty, without aiming our attention to copula/marginals inference. Instead, we studied the

effect of additional flood information not only on the distribution parameters but also on the uncertainty range in a Bayesian framework that among else permits the consideration of errors from different sources.

The extra flood data that included additional peaks from different hydrometric stations leaded to a peak distribution with bigger mean and smaller shape parameters and thus to elevated peaks, since it includes flood events of recent years that exceed in magnitude the events of the historical data series. Consequently, including the additional information translates into a general bigger estimate of the peaks, which is also reflected on the MWL's, as the peak is a driving factor of the routing process.

The uncertainty range of discharge and volume is considerable and affects, along with the copula parameter, the MWL. The variations in the MWL for the same structure-based return period correspond to significant variation in the stored water volume. Most importantly, the return period of a specific water level cannot be determined with certainty because the return periods of the events overlap. Naturally, the range of discharge and volume values for a given structure-based return period is very ample due to the wide range of the parameters of the inferred distributions.

A clear observation of whether uncertainty is systematically reduced with the introduction of additional information cannot be made, here. Nonetheless, a Bayesian framework allows a certain degree of transparency (Parkes and Demeritt, 2016). Incorporating knowledge about water levels during historic events, e.g. at the locality of Navicello for the 1783 and 1842 flood, could result in a more significant change in the uncertainty range, as past researches have shown. But, one must consider also the great amount of error involved in these data in the Bayesian framework.

As a general remark one can deduce that the process of risk estimation is inherently crippled by uncertainty that can be quantified or at least approximated. Any attempt to obscure this uncertainty could create a false notion about its existence in a multivariate problem with eventual implications in dam safety.

Data availability

The dataset used in this research is available upon request from the corresponding author.

The authors declare that they have no conflict of interest.

Acknowledgements. We would like to thank Dr. Francesco Serinaldi and an anonymous referee for their instructive comments. We would also like to thank Stefano Orlandini for providing us with all the information regarding the Panaro dam. For the routing of the hydrographs we used the model developed by Gambarelli et al. (2009).

The analysis was implemented in R Statistical Computing Software (R Core Team, 2015) with the use of the following contributed packages: CDVine (Brechmann and Schepsmeier, 2013), Cairo (Urbanek and Horner, 2015), copula (Kojadinovic and Yan, 2010; Yan, 2007), fitdistrplus (Delignette-Muller and Dutang, 2015), goftest (Faraway et al., 2015), hdrcde (Rob J Hyndman with contributions from Jochen Einbeck and Matt Wand, 2013), ks (Duong, 2016), LaplacesDemon (Statisticat, LLC, 2016), lmomco (Asquith, 2015), statmod (Smyth et al., 2015), VGAM (Yee, 2010), wordcloud (Fellows, 2014).

References

Ariff, N. M., Jemain, A. A., Ibrahim, K., and Wan Zin, W. Z.: IDF relationships using bivariate copula for storm events in Peninsular Malaysia, Journal of Hydrology, 470–471, 158–171, doi:http://dx.doi.org/10.1016/j.jhydrol.2012.08.045, 2012.

Aronica, G. T., Candela, A., Fabio, P., and Santoro, M.: Estimation of flood inundation probabilities using global hazard indexes based on hydrodynamic variables, Physics and Chemistry of the Earth, Parts A/B/C, 42–44, 119–129, doi:http://dx.doi.org/10.1016/j.pce.2011.04.001, 2012.

Asquith, W.: lmomco—L-moments, censored L-moments, trimmed L-moments, L-comoments, and many distributions, http://www.cran.r-project.org/package=lmomco, r package version 2.1.4, 2015.

Autorità di bacino del fiume Po: Caratteristiche del bacino del fiume Po e primo esame dell'impatto ambientale delle attività umane sulle risorse idriche, Report (in Italian), 2006.

Balistrocchi, M. and Bacchi, B.: Modelling the statistical dependence of rainfall event variables through copula functions, Hydrol. Earth Syst. Sci., 15, 1959–1977, doi:10.5194/hess-15-1959-2011, 2011.

Balistrocchi, M., Ranzi, R., and Bacchi, B.: Multivariate Statistical Analysis of Flood Variables by Copulas: Two Italian Case Studies, in: 3rd IAHR Europe Congress, 2014.

Brechmann, E. C. and Schepsmeier, U.: Modeling Dependence with C- and D-Vine Copulas: The R Package CDVine, Journal of Statistical Software, 52, 27, doi:10.18637/jss.v052.i03, 2013.

Burnham, K. P. and Anderson, D. R.: Multimodel inference understanding AIC and BIC in model selection, Sociological methods research, 33.2, 261–304, 2004.

Candela, A., Brigandì, G., and Aronica, G. T.: Estimation of synthetic flood design hydrographs using a distributed rainfall–runoff model coupled with a copula-based single storm rainfall generator, Nat. Hazards Earth Syst. Sci., 14, 1819–1833, doi:10.5194/nhess-14-1819-2014, 2014.

De Michele, C. and Rosso, R.: A multi-level approach to flood frequency regionalisation, Hydrol. Earth Syst. Sci., 6, 185–194, doi:10.5194/hess-6-185-2002, 2002.

De Michele, C. and Salvadori, G.: A Generalized Pareto intensity-duration model of storm rainfall exploiting 2-Copulas, Journal of Geophysical Research: Atmospheres, 108, n/a–n/a, doi:10.1029/2002JD002534, 2003.

De Michele, C., Salvadori, G., Canossi, M., Petaccia, A., and Rosso, R.: Bivariate Statistical Approach to Check Adequacy of Dam Spillway, Journal of Hydrologic Engineering, 10, 50–57, doi:doi:10.1061/(ASCE)1084-0699(2005)10:1(50), 2005.

Delignette-Muller, M. L. and Dutang, C.: fitdistrplus: An R Package for Fitting Distributions, 2015, 64, 34, doi:10.18637/jss.v064.i04, 2015.

Domeneghetti, A., Vorogushyn, S., Castellarin, A., Merz, B., and Brath, A.: Probabilistic flood hazard mapping: effects of uncertain boundary conditions, Hydrol. Earth Syst. Sci., 17, 3127–3140, doi:10.5194/hess-17-3127-2013, 2013.

Dung, N. V., Merz, B., Bárdossy, A., and Apel, H.: Handling uncertainty in bivariate quantile estimation – An application to flood hazard analysis in the Mekong Delta, Journal of Hydrology, 527, 704–717, doi:http://dx.doi.org/10.1016/j.jhydrol.2015.05.033, 2015.

Duong, T.: ks: Kernel Smoothing, http://CRAN.R-project.org/package=ks, r package version 1.10.4, 2016.

Durante, F. and Sempi, C.: Principles of copula theory, CRC Press, 2015.

Dyck, S. and Peschke, G.: Grundlagen der Hydrologie, Verlag für Bauwesen, Berlin, 1995.

Faraway, J., Marsaglia, G., Marsaglia, J., and Baddeley, A.: goftest: Classical Goodness-of-Fit Tests for Univariate Distributions, http://CRAN.R-project.org/package=goftest, r package version 1.0-3, 2015.

Fellows, I.: wordcloud: Word Clouds, http://CRAN.R-project.org/package=wordcloud, r package version 2.5, 2014.

Frahm, G., Junker, M., and Schmidt, R.: Estimating the tail-dependence coefficient: Properties and pitfalls, Insurance: Mathematics and Economics, 37, 80–100, doi:http://dx.doi.org/10.1016/j.insmatheco.2005.05.008, 2005.

Gambarelli, P., Moretti, G., and Orlandini, S.: Sviluppo di un Modello Matematico del Funzionamento Idraulico della Cassa di Espansione sul Fiume Panaro, Thesis, 2009.

Ganguli, P. and Reddy, M. J.: Probabilistic assessment of flood risks using trivariate copulas, Theoretical and Applied Climatology, 111, 341–360, doi:10.1007/s00704-012-0664-4, 2013.

Gaume, E., Gaál, L., Viglione, A., Szolgay, J., Kohnová, S., and Blöschl, G.: Bayesian MCMC approach to regional flood frequency analyses involving extraordinary flood events at ungauged sites, Journal of Hydrology, 394, 101–117, doi:http://dx.doi.org/10.1016/j.jhydrol.2010.01.008, 2010.

Genest, C. and Favre, A.: Everything You Always Wanted to Know about Copula Modeling but Were Afraid to Ask, Journal of Hydrologic Engineering, 12, 347–368, doi:10.1061/(ASCE)1084-0699(2007)12:4(347), 2007.

Gräler, B., van den Berg, M. J., Vandenberghe, S., Petroselli, A., Grimaldi, S., De Baets, B., and Verhoest, N. E. C.: Multivariate return periods in hydrology: a critical and practical review focusing on synthetic design hydrograph estimation, Hydrol. Earth Syst. Sci., 17, 1281–1296, doi:10.5194/hess-17-1281-2013, 2013.

Halbert, K., Nguyen, C. C., Payrastre, O., and Gaume, E.: Reducing uncertainty in flood frequency analyses: A comparison of local and regional approaches involving information on extreme historical floods, Journal of Hydrology, 541, Part A, 90–98, doi:http://dx.doi.org/10.1016/j.jhydrol.2016.01.017, 2016.

Hyndman, R. J.: Computing and Graphing Highest Density Regions, The American Statistician, 50, 120–126, doi:10.2307/2684423, 1996.

Joe, H.: Dependence modeling with copulas, CRC Press, 2014.

Kojadinovic, I. and Yan, J.: Modeling Multivariate Distributions with Continuous Margins Using the copula R Package, Journal of Statistical Software, 34, 20, doi:10.18637/jss.v034.i09, 2010.

Merz, R. and Blöschl, G.: Flood frequency hydrology: 1. Temporal, spatial, and causal expansion of information, Water Resources Research, 44, n/a–n/a, doi:10.1029/2007WR006744, 2008.

Nelsen, R. B.: An introduction to copulas, vol. 139, Springer Science Business Media, 2006.

Nora, E. and Ghinoi, A.: Alluvioni e terremoti: Principali rischi naturali di Modena nel Novecento, http://www.comune.modena.it/lecittasostenibili/documenti-cittasostenibili/annale-900-citt-ambiente/alluvioni-e-terremoti, 2009.

Ouarda, T. B. M. J. and El-Adlouni, S.: Bayesian Nonstationary Frequency Analysis of Hydrological Variables1, JAWRA Journal of the American Water Resources Association, 47, 496–505, doi:10.1111/j.1752-1688.2011.00544.x, 2011.

Parent, E. and Bernier, J.: Encoding prior experts judgments to improve risk analysis of extreme hydrological events via POT modeling, Journal of Hydrology, 283, 1–18, doi:http://dx.doi.org/10.1016/S0022-1694(03)00080-5, 2003.

Parkes, B. and Demeritt, D.: Defining the hundred year flood: A Bayesian approach for using historic data to reduce uncertainty in flood frequency estimates, Journal of Hydrology, 540, 1189–1208, doi:http://dx.doi.org/10.1016/j.jhydrol.2016.07.025, 2016.

R Core Team: R: A Language and Environment for Statistical Computing, R Foundation for Statistical Computing, Vienna, Austria, http://www.R-project.org/, 2015.

Reis Jr, D. S. and Stedinger, J. R.: Bayesian MCMC flood frequency analysis with historical information, Journal of Hydrology, 313, 97–116, doi:http://dx.doi.org/10.1016/j.jhydrol.2005.02.028, 2005.

Requena, A. I., Mediero, L., and Garrote, L.: A bivariate return period based on copulas for hydrologic dam design: accounting for reservoir routing in risk estimation, Hydrol. Earth Syst. Sci., 17, 3023–3038, doi:10.5194/hess-17-3023-2013, 2013.

Rob J Hyndman with contributions from Jochen Einbeck and Matt Wand: hdrcde: Highest density regions and conditional density estimation, http://CRAN.R-project.org/package=hdrcde, r package version 3.1, 2013.

Salvadori, G. and De Michele, C.: On the Use of Copulas in Hydrology: Theory and Practice, Journal of Hydrologic Engineering, 12, doi:doi:10.1061/(ASCE)1084-0699(2007)12:4(369), 2007.

Salvadori, G., De Michele, C., Kottegoda, N., and Rosso, R.: Extremes in Nature: An Approach Using Copulas, Water Science and Technology Library, Springer Netherlands, 1 edn., doi:10.1007/1-4020-4415-1, 2007.

Salvadori, G., Durante, F., Tomasicchio, G. R., and D'Alessandro, F.: Practical guidelines for the multivariate assessment of the structural risk in coastal and off-shore engineering, Coastal Engineering, 95, 77–83, doi:http://dx.doi.org/10.1016/j.coastaleng.2014.09.007, 2015.

Schmidt, R. and Stadtmüller, U.: Non-parametric Estimation of Tail Dependence, Scandinavian Journal of Statistics, 33, 307–335, doi:10.1111/j.1467-9469.2005.00483.x, 2006.

Serinaldi, F.: An uncertain journey around the tails of multivariate hydrological distributions, Water Resources Research, 49, 6527–6547, doi:10.1002/wrcr.20531, 2013.

Serinaldi, F.: Can we tell more than we can know? The limits of bivariate drought analyses in the United States, Stochastic Environmental Research and Risk Assessment, 30, 1691–1704, doi:10.1007/s00477-015-1124-3, 2016.

Serinaldi, F., Bárdossy, A., and Kilsby, C. G.: Upper tail dependence in rainfall extremes: would we know it if we saw it?, Stochastic Environmental Research and Risk Assessment, 29, 1211–1233, doi:10.1007/s00477-014-0946-8, 2015.

Servizio Idrografico Italiano: Dati Caratteristici dei Corsi d'Aqcua Italiani, Ministero dei Lavori Pubblici- Istituto Poligrafico dello Stato, In Italian, 1939,1953.

Singh, V. P.: Effect of spatial and temporal variability in rainfall and watershed characteristics on stream flow hydrograph, Hydrological Processes, 11, 1649–1669, doi:10.1002/(SICI)1099-1085(19971015)11:12<1649::AID-HYP495>3.0.CO;2-1, 1997.

Singh, V. P. and Zhang, L.: IDF Curves Using the Frank Archimedean Copula, Journal of Hydrologic Engineering, 12, 651–662, doi:doi:10.1061/(ASCE)1084-0699(2007)12:6(651), 2007.

Sklar, M.: Fonctions de répartition à n dimensions et leurs marges, Université Paris 8, 1959.

Smyth, G., Hu, Y., Dunn, P., Phipson, B., and Chen, Y.: statmod: Statistical Modeling, http://CRAN.R-project.org/package=statmod, r package version 1.4.21, 2015.

Statisticat, LLC: LaplacesDemon: Complete Environment for Bayesian Inference, https://cran.r-project.org/web/packages/LaplacesDemon/, r package version 16.0.1, 2016.

Urbanek, S. and Horner, J.: Cairo: R graphics device using cairo graphics library for creating high-quality bitmap (PNG, JPEG, TIFF), vector (PDF, SVG, PostScript) and display (X11 and Win32) output, http://CRAN.R-project.org/package=Cairo, r package version 1.5-9, 2015.

Viglione, A., Merz, R., Salinas, J. L., and Blöschl, G.: Flood frequency hydrology: 3. A Bayesian analysis, Water Resources Research, 49, 675–692, doi:10.1029/2011WR010782, 2013.

Volpi, E. and Fiori, A.: Hydraulic structures subject to bivariate hydrological loads: Return period, design, and risk assessment, Water Resources Research, 50, 885–897, doi:10.1002/2013WR014214, 2014.

Yan, J.: Enjoy the Joy of Copulas: With a Package copula, 2007, 21, 21, doi:10.18637/jss.v021.i04, 2007.

Yee, T. W.: The VGAM Package for Categorical Data Analysis, 2010, 32, 34, doi:10.18637/jss.v032.i10, 2010.

Zhang, L. and Singh, V. P.: Bivariate rainfall frequency distributions using Archimedean copulas, Journal of Hydrology, 332, 93–109, doi:10.1016/j.jhydrol.2006.06.033, 2007.

Zhang, Q., Xiao, M., and Singh, V. P.: Uncertainty evaluation of copula analysis of hydrological droughts in the East River basin, China, Global and Planetary Change, 129, 1–9, doi:http://dx.doi.org/10.1016/j.gloplacha.2015.03.001, 2015.

Table 1. Main hydrological characteristics of the Panaro watershed (area A, main stream length L, minimum elevation H_{min}, elevation drop ΔH, time of concentration t_c).

A [km^2]	876
L [km]	124.4
H_{min} [m]	32
ΔH [m]	1449.9
t_c [h]	10.0

Table 2. Estimated parameters of the inferred distributions and their confidence interval (95%).

	Parameter name	Estimated parameter	Confidence interval (95%)	Standard deviation
Gumbel-Hougaard	θ	2.27	[1.79,3.01]	0.38
Inverse Gaussian for peak (single site)	μ	364.12	[323.64,416.40]	23.67
	λ	1957.16	[1288.05,2820.61]	380.17
Inverse Gaussian for peak (multi-site &	μ	398.61	[358.42,442.54]	21.89
historical information)	λ	1533.41	[1108.84,2058.99]	256.37
Rayleigh for volume	σ	386.58×10^5	$[343.18,430.53]\times10^5$	26.54×10^5

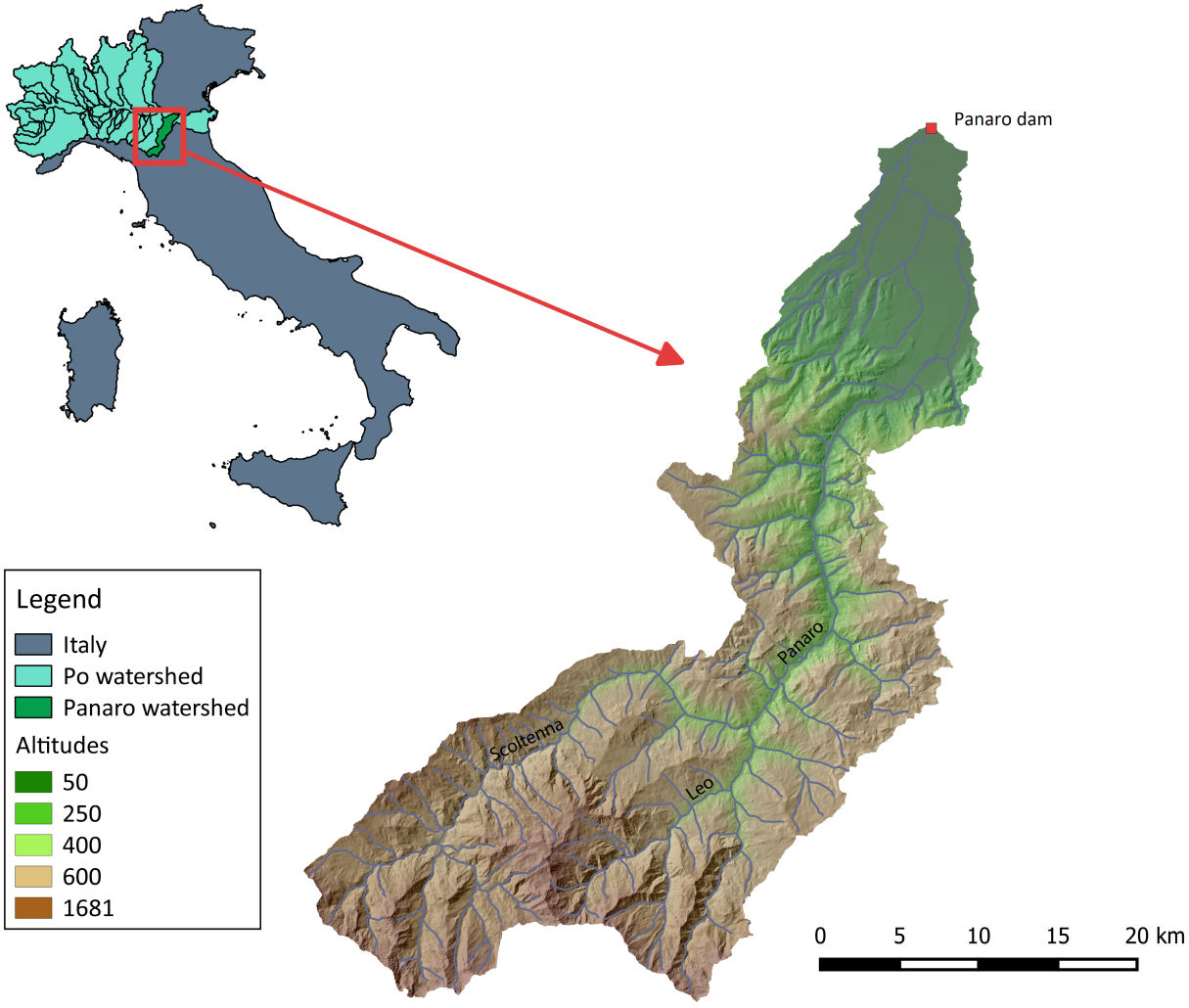

Figure 1. Panaro study watershed

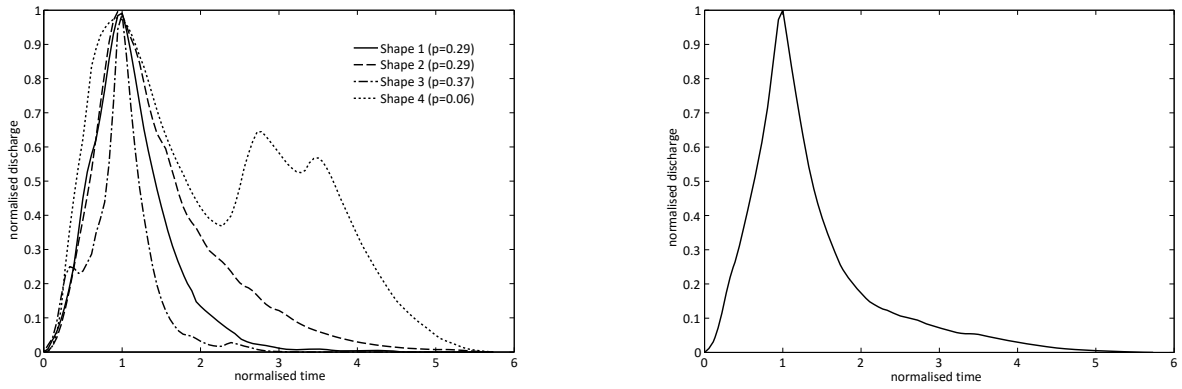

Figure 2. Characteristic normalised hydrograph shapes (a) with a certain probability of occurrence; (b) "Mean" normalised hydrograph shape.

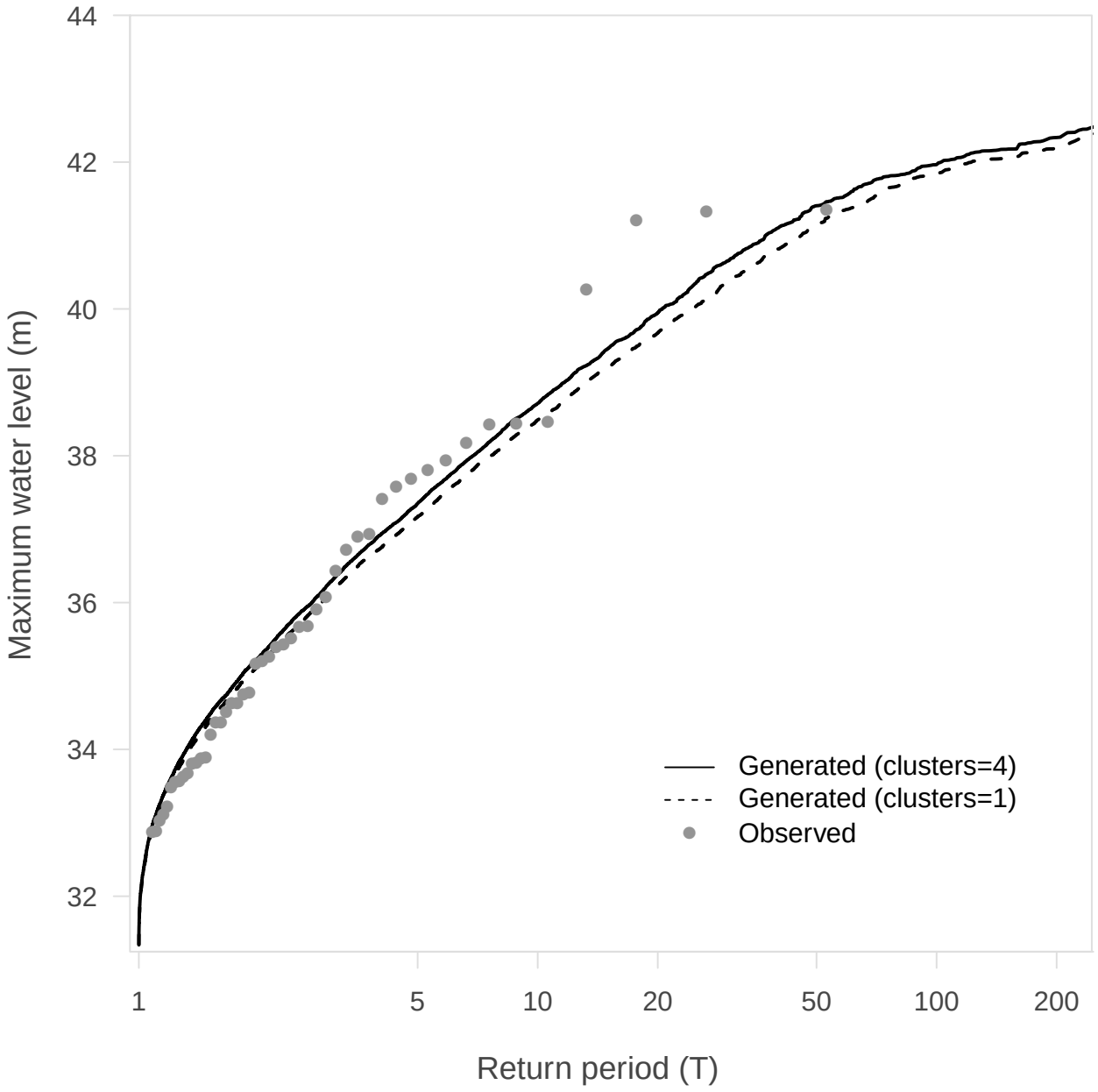

Figure 3. Frequency curves of maximum water level of synthetic hydrographs for four clusters and one cluster and corresponding levels of observed hydrographs.

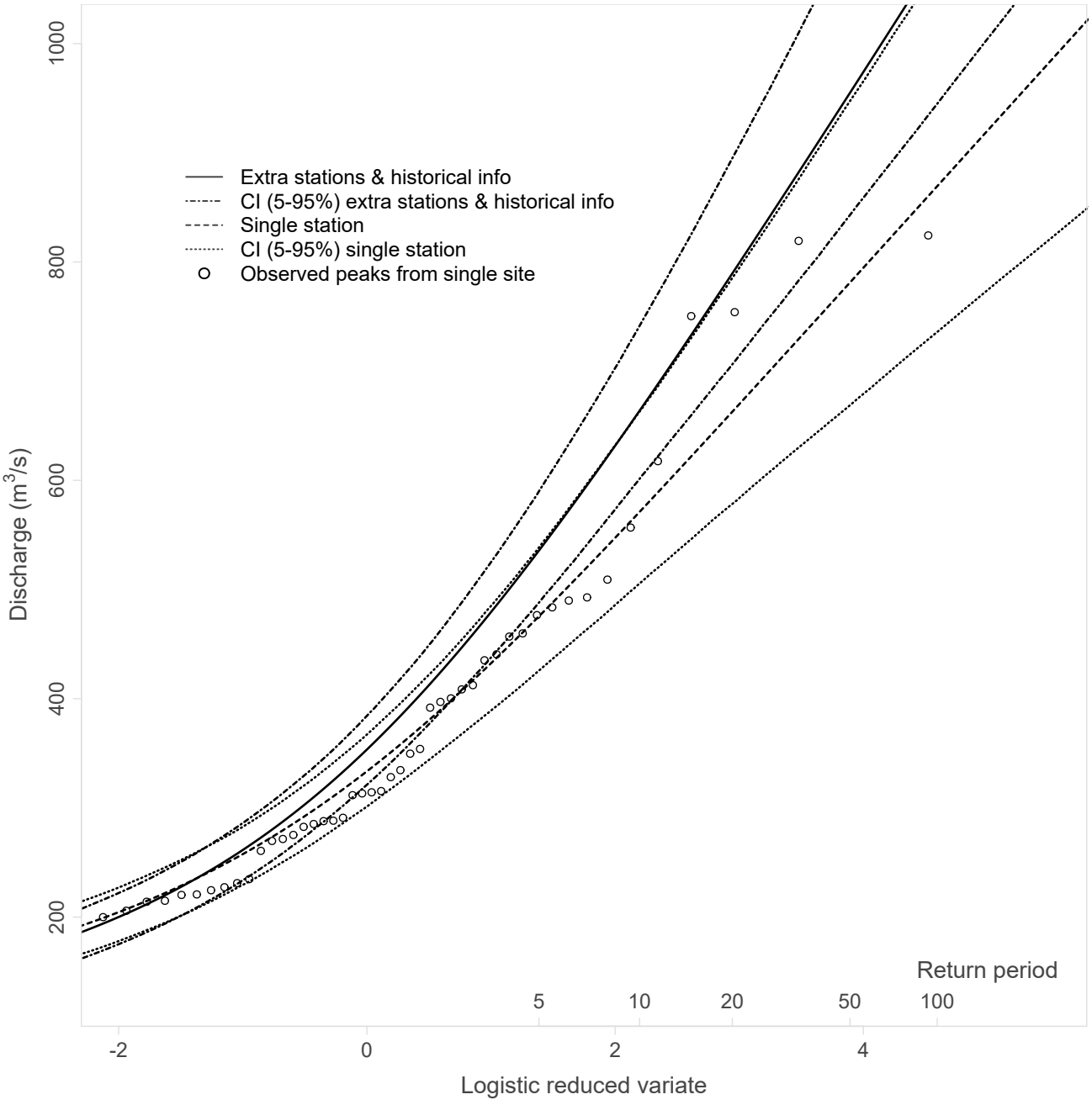

Figure 4. Flood frequency curves with 95 % confidence limits for the single-site data and the multi-site data with extra information case. Observed peaks are also plotted with the Gringorten plotting position.

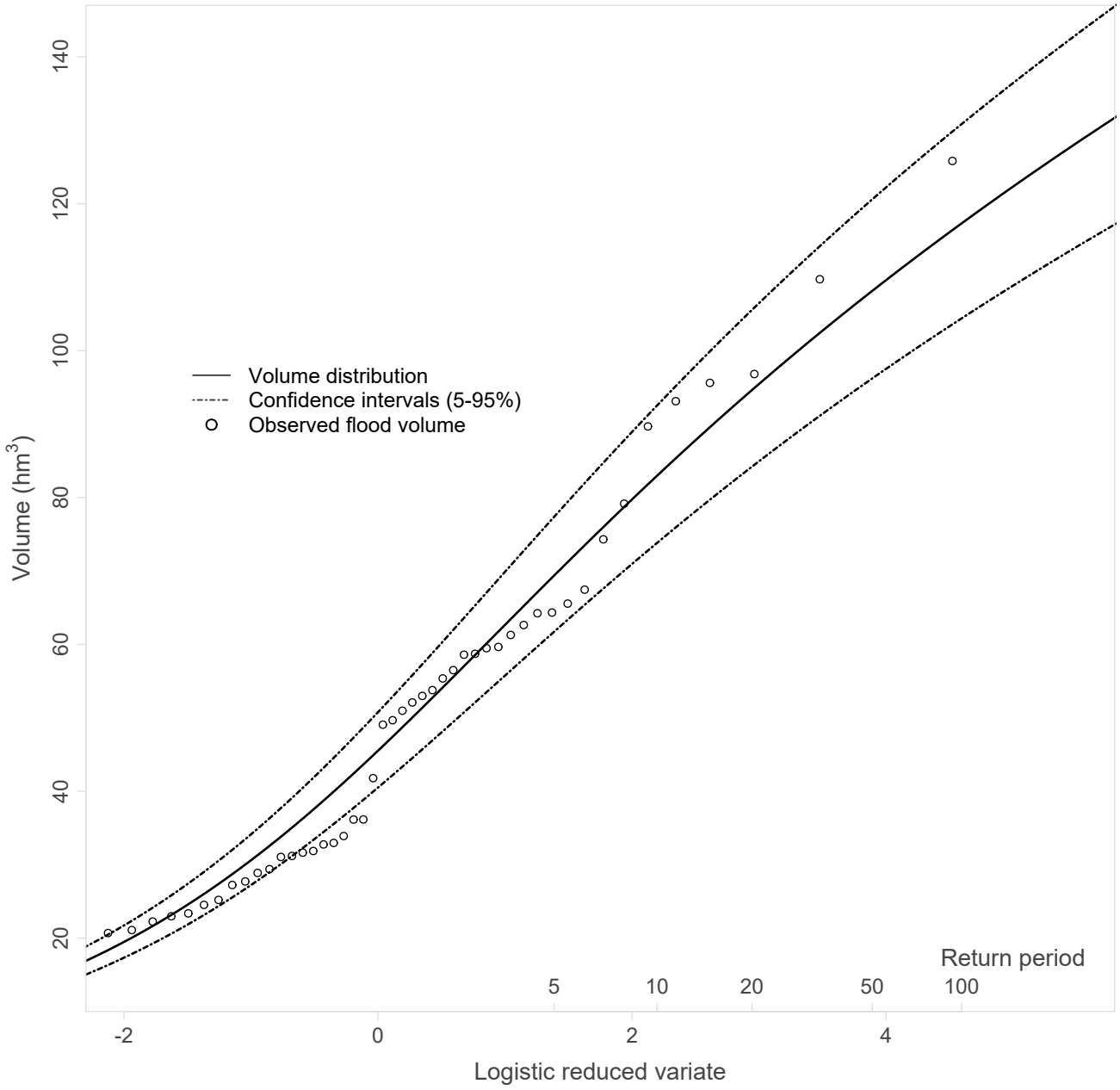

Figure 5. Flood volume curve with 95 % confidence limits. Observed flood volumes are also plotted with the Gringorten plotting position.

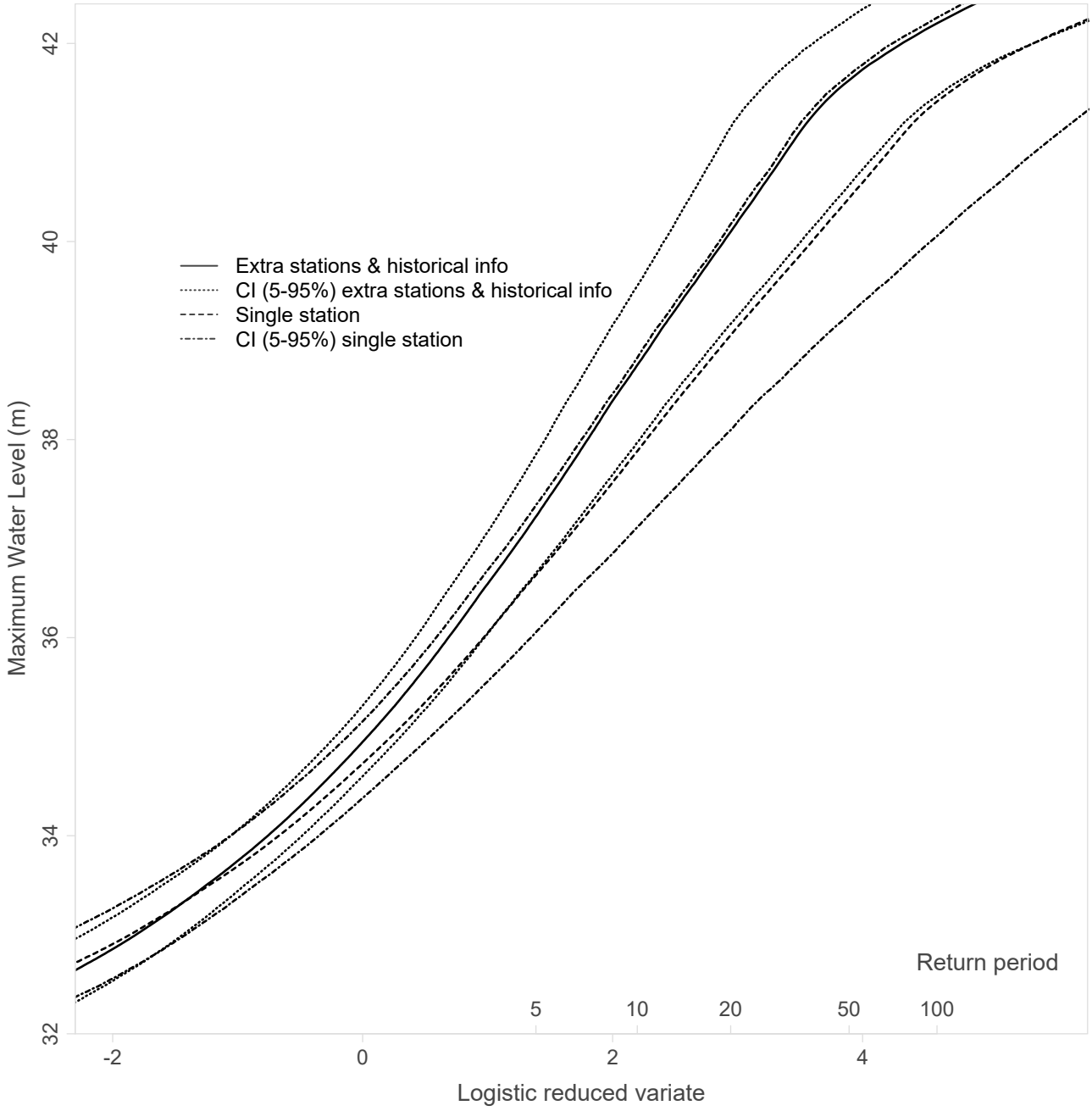

Figure 6. MWL frequency curves with 95 % confidence limits for the single-site data and the multi-site data with extra information case.

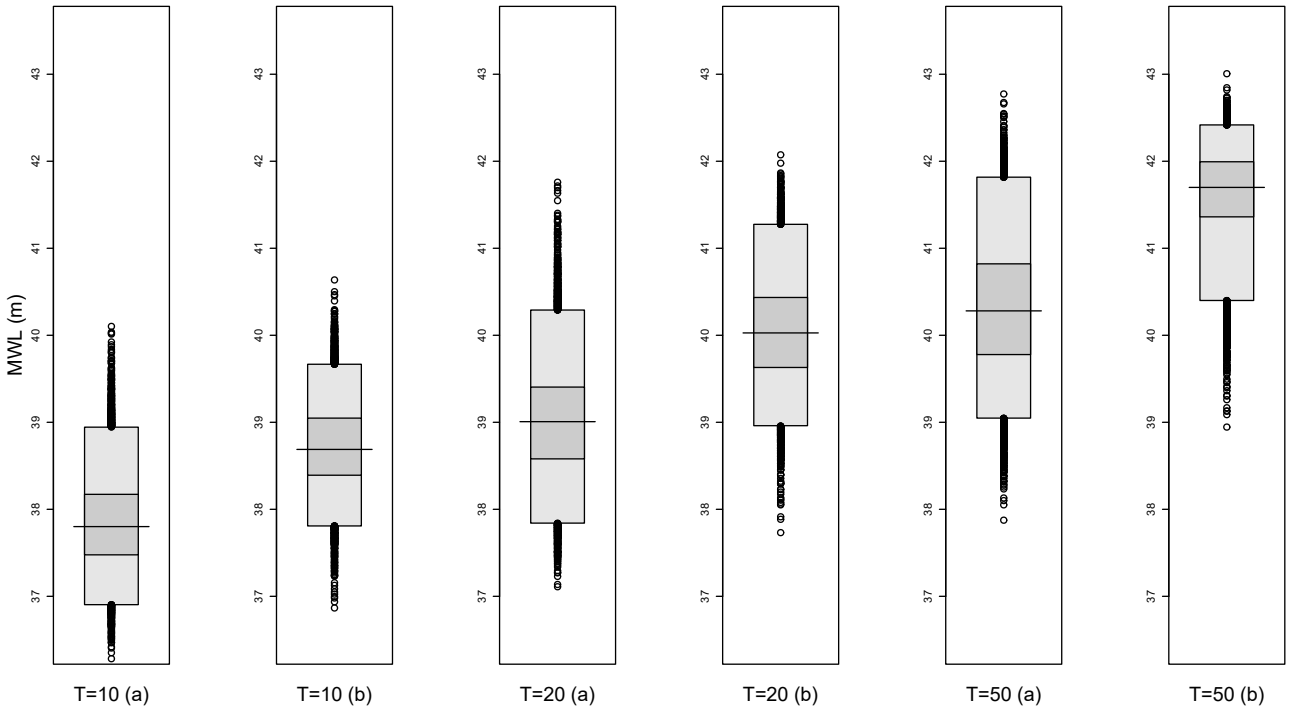

Figure 7. High density region boxplots of MWL for return periods of 10, 20 and 50 years for (a) single-site data and (b) multi-site data with historical information.

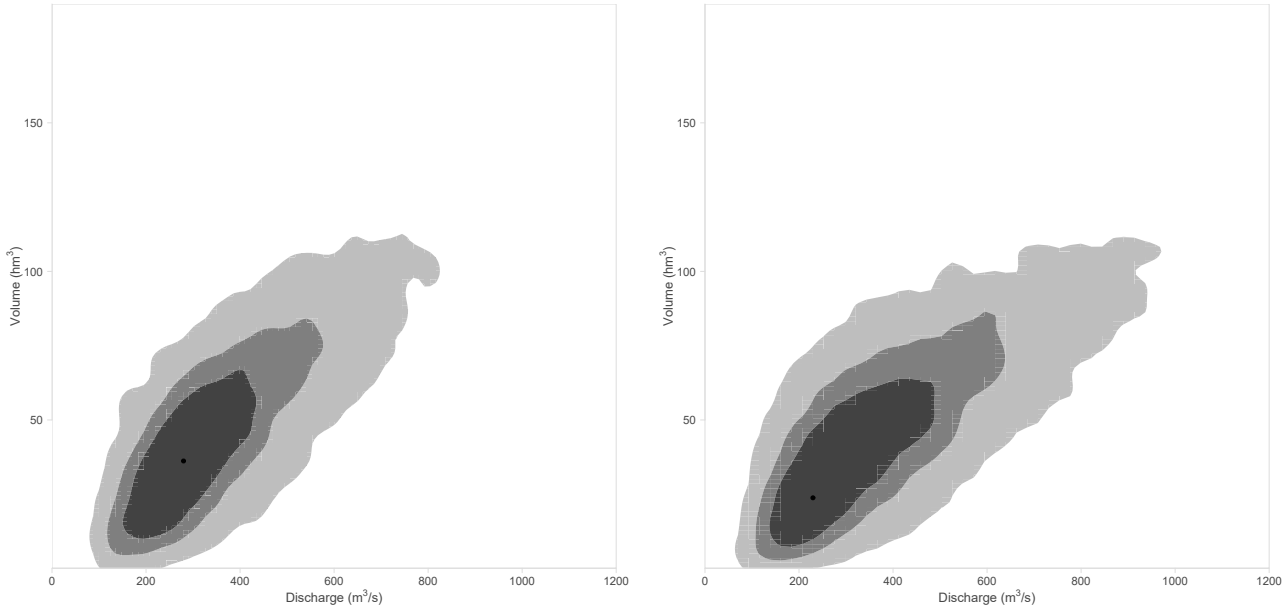

Figure 8. 50, 75 and 95 % of the kernel density areas of MWL's with a return period of 50 years on the discharge-volume plane, for single-site data (a) and multi-site data with historical information (b).